Journal of The Electrochemical Society, **153** (8) D138-D142 (2006)
0013-4651/2006/153(8)/D138/5/$20.00 © The Electrochemical Society

Ferromagnetism at Room Temperature on Electrodeposited Co^{2+}-Doped ZnO Thin Film

M. Abid,[a,z] J.-P. Abid,[b] and J.-Ph. Ansermet[a]

[a]*EPFL/Institut de Physique des Nanostructures, and* [b]*EPFL/ISIC, Lausanne CH-1015, Switzerland*

Predicted by the theory, ferromagnetism is expected in Co-doped ZnO. Recently, ferromagnetism above room temperature was reported in thin films as well as in bulk samples made of cobalt-doped zinc oxide. In this study, we report the preparation of ZnO doped with ~5% of Co ($Zn_{1-x}Co_xO$, $x = 0.05$) by electrodeposition. Sample characterization using X-ray diffraction, high-resolution transmission electron microscopy, and X-ray photoelectron spectroscopy shows that the dopant is substitutional. Moreover, the magnetic properties of Co-doped ZnO samples electrodeposited as a function of field and temperature exhibit clearly ferromagnetism with Curie temperature above 400 K.
 [DOI: 10.1149/1.2207839]

Manuscript submitted December 6, 2005; revised manuscript received April 10, 2006. Available electronically June 13, 2006.

In recent years, ferromagnetism in semiconductors has attracted significant attention partly due to interest in spintronic device concepts.[1-3] In the year 2000, Dietl et al.[4] made the theoretical prediction that Mn-doped ZnO and GaN would be ferromagnetic at room temperature and would therefore be suitable for applications in spintronics. Similar theoretical calculations of Sato and Katayama-Yoshida[5] showed that ZnO doped with several three-dimensional (3D) transition metal ions such as V, Cr, Fe, Co, and Ni may exhibit ferromagnetic ordering. Much of the recent effort has focused on conventional II–VI and III–V semiconductor materials. A report of ferromagnetism in Co-doped TiO_2 gave the hope that Co- and Mn-doped oxides may indeed be useful for spintronics.[6] Recently, low-temperature epitaxial growth has been used with Mn-doped ZnO in achieving ferromagnetism, showing a transition temperature of 470 K which is the highest T_C[7] for doped semiconductor. They have also found that on heating the bulk samples above 875 K, the ferromagnetic content of the sample decreases, which they attributed to the clustering of Mn. Ferromagnetism in these materials operates via a mechanism by which itinerant carriers are spin polarized and mediate ferromagnetic ordering between the widely spaced dopant ions (RKKY interaction) when localized spin is introduced in the oxide semiconductor. The oxidation state (and spin state), homogeneity and substitutional incorporation of the dopant must be considered when transition metal is doped for producing dilute magnetic semiconductors. In this case, the heating process increases the possibility of inadvertently altering the oxidation state of the dopants.[8]

In this paper, an electrodepositing technique for the preparation of one phase ZnO thin film doped with 2 to 6% of Co is detailed (low temperature process). The magnetic investigation shows that the prepared films present a ferromagnetic behavior for a temperature higher than room temperature. Some salient features of using electrodeposition instead of the thermal method to produce ferromagnetic semiconductor are: low cost, simplicity, possibility of using starting materials of high purity.

Experimental

The $Zn_{1-x}CoO$ synthesis was achieved through the co-precipitation method. Typically, the electrodeposition experiment was carried out in a classical three electrode glass cell. Two different working electrodes have been employed, a gold layer/adhesive chromium layer deposited on a silicon (100) wafer , or polycrystalline gold layer. The electrode is sonicated in a distilled water bath for 5 min to remove dust from the surface. Finally, the electrode is washed with Milli-Q water (0.82 μS/cm). The circuit loop is closed using a satured Ag/AgCl electrode as reference and a platinum wire as counter electrode. The potential window is estimated using cyclic voltammetry (CV). All the experiments were performed at 343 K under N_2 bubbling for at least 1 h and employing the EG 273A potentiostatic system. The electrodeposition was carried out in aqueous solution composed of 3 g/L $ZnCl_2$ (supplied by Merck, 99.999%), 1 g/L of $NaNO_3$, and a different concentration $CoSO_4$ (supplied by Fluka, 99.99%) at pH 5.5 to avoid any formation of precipitate. After each electrodeposition, the sample was washed with distilled water to remove the Zn^{2+} and Co^{2+} left from the electrodeposition solution.

The structural characterization of the material was investigated using X-ray microanalysis mapping, X-ray diffraction scanning electron microscopy (XRD-SEM) and high-resolution transmission electron microscopy (HRTEM). HRTEM analysis was carried out on a Philips CM300 Bragg-Brentano diffractometer operating at the Cu Kα wavelength (1.542 Å) in the θ–2θ Bragg configuration. The voltage was set at 50 kV with a 45 mA flux. SEM images were obtained using a Philips XL30 field emission gun (FEG) microscope. The X-ray photoelectron microscopy (XPS) was obtained using an ESCA QUANTUM 2000. The photoelectron emitted by radiation of a monochromated Mg Kα (1256.6 eV, 200 W) source, having a fixed path energy of 11.75 eV, were collected at a multichannel detector through a hemispherical analyzer. Before each acquisition we sputtered some ion argon to ensure that the surface is free from residual Co^{2+} and Zn^{2+} that might have remained even after washing many times with water and ethanol. Theoretical curves were adjusted to fit the peaks by means of an in-house computer program. A Doniach-Sunjic Lorentzian asymmetric function[9] was convoluted with an experimental Gaussian curve (G = 0.8) and a Shirley background[10] was subtracted. A quantum design MPMS5 superconducting quantum interference device (SQUID) magnetometer was used to determine the magnetic properties of the $Zn_{1-x}Co_xO$ ($x = 0.05$) samples. The measurement temperature of SQUID can be varied from 1.7 to 400 K and the field can go up to 5 T.

Results and Discussion

Cyclic voltammogramms.— Figure 1 shows the CV as a function of potential for a solution of 3 g/L $ZnCl_2$, 3 g/L of $NaNO_3$, and 3 g/L of $CoSO_4$ at pH 5.5. We observe a small increase of the cathodic current reduction from approximately −0.5 V. This increase can be related to the reduction of NO_3^- dissolved in the solution into OH^- (Eq. 1) as proposed by Lincot.[11] The increase at −1 V, can either be due to the formation reduced cobalt ion from the electrolyte[12] and/or by reduction of $Co(OH)_2$ as reported by Foelske et al.[13] The formation of metallic cobalt is corroborated by XPS and TEM analysis. After reversing the potential at −1.2 V, the cobalt reduction proceeds up to −0.95 V. The cobalt dissolution process begins at −0.9 V which is characterized by an anodic current peak.

$$NO_3^- + 2e^- + H_2O \rightarrow 2OH^- + NO_2^- \quad [1]$$

$$M + 2OH^- \rightarrow M(OH)_2 \quad [2]$$

[z] E-mail: mohamed.abid@epfl.ch

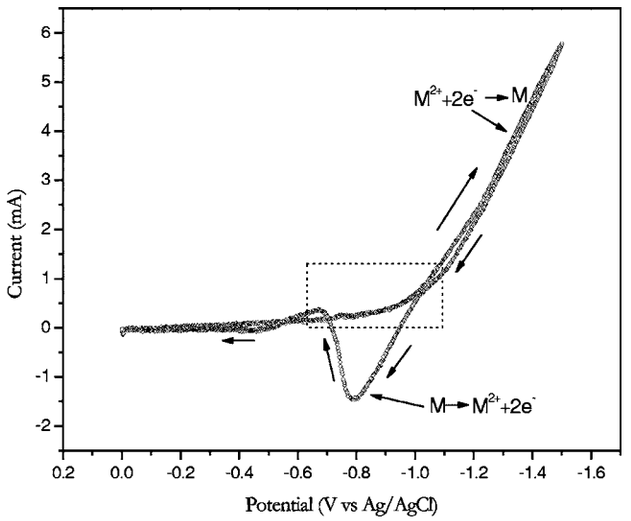

Figure 1. CV as a function of potential measured in a solution containing 3 g/L $ZnCl_2$, 3 g/L of $Co(SO_4)_2$, and 1 g $NaNO_3$ at 343 K, scan rate 100 mV/s^{-1}, pH 5.5.

$$M(OH)_2 \rightarrow ZnCo_xO_{1-x} + H_2O \ (M = Zn,Co)(343\ K) \qquad [3]$$

The second reaction, corresponding to the formation of $Zn(OH)_2$ and $Co(OH)_2$, is a precipitation reaction taking place on the surface, due to the local increase of pH. At 343 K, the co-precipitation of $Zn(OH)_2$ and $Co(OH)_2$ form $Zn_{1-x}Co_xO$ following the chemical reaction. We observe that to reach a reasonable deposition rate of $Zn(OH)_2$ and $Co(OH)_2$, the applied potential vs the silver/silver chloride reference must be at least equal or up to −0.8 V and below −0.95 V. Moreover, this potential range avoids the formation of Co metallic clusters. Figure 2a shows the energy dispersive spectra of characteristic Co Kα peaks at 6.9 eV. Figure 2b summarizes the content of Co in doped ZnO vs the concentration Co^{2+} (g/L) into the electrolyte. This elemental composition for $Co_xZn_{1-x}O$ was determined by XPS.

Structural characterization.— Figure 3a is a SEM of the polycrystalline film on the gold surface. No preferred orientation of the structure is observed. On gold layer Au{111} (Fig. 3b), undoped and doped ZnO with Co, shows a well oriented hexagonal structure perpendicular to the substrate with a bimodal size distribution located at 300 and 100 nm. It must be pointed out that 2 h of electrodeposition is necessary to obtain nonporous films. In that regime, it appears that the grains merge intimately together. On this sample the density of grain is $\sim 6 \times 10^8$ cm^2 and the vertical growth is ~0.6 μm/h.

Pauporte and Lincot[14] have shown that epitaxial films of ZnO can be electrodeposited onto single-crystal gallium nitride. More recently, Switzer and his collaborators were the pioneers to report an epitaxial growth of ZnO onto cubic Au{111}, Au{110}, and Au{100} single-crystal substrates. The result obtained on gold {111} is in good agreement with the results observed by Switzer.[15] Figure 4 displays the XRD of a 5% Co-doped ZnO, two peaks at $2\theta = 34.1°$ and $2\theta = 38.2°$ were observed, corresponding to ZnO{002} and Au{111}, respectively. Using the XRD linewidth, an average nanocrystallite size of ~110 nm is estimated. The value obtained is in good agreement with the SEM observations. The XRD pattern demonstrates highly crystallized wurtzite and is essentially identical to those of bulk ZnO. Furthermore, from the ZnO{002} peak position, the lattice parameter, a, is estimated to be 3.289 Å. The experimental value is 1.3% larger than that of pure würtzite (3.250 Å) and is most likely due to the substitution of the larger Co^{+2} ion for Zn^{+2},

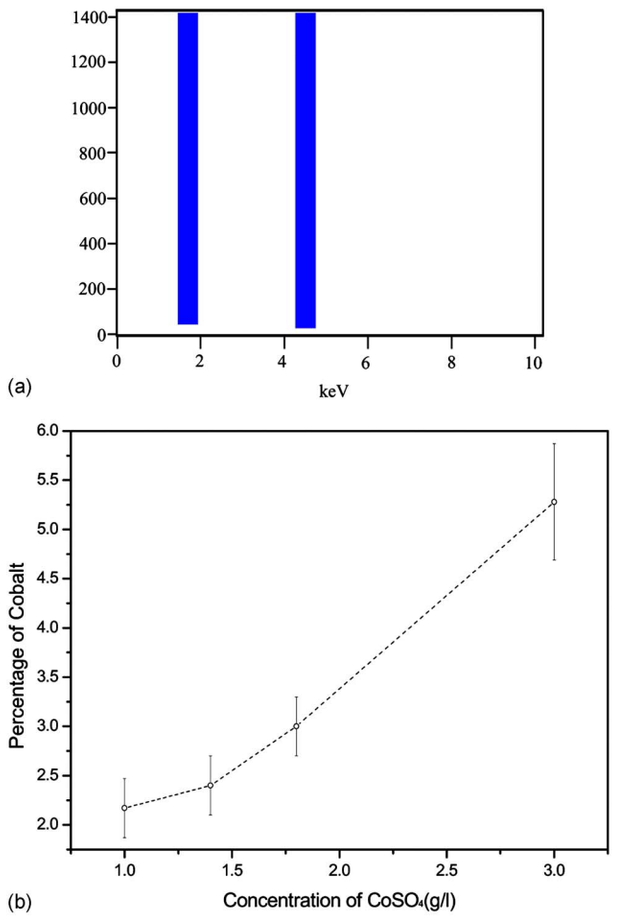

Figure 2. (a) Typical EDS spectra of $Co_xZn_{1-x}Co$ ($x = 0.05$). (b) Percentage of cobalt doped in ZnO vs the concentration of $CoSO_4$ (g/L)

meaning that Co is either present in negligible amounts or was substitutionally doped into the ZnO crystal structure to form a solid solution.[16]

To identify the homogeneity distribution of Co in the electrodeposited film, Energy dispersive spectrometry (EDS) mapping of Zn and Co is made on different areas and at different magnifications (not shown). We observe no segregation phase of cobalt (only one phase) is observed. To determine the charge state of Co in the film, XPS measurements have been performed on the sample. Figure 5a shows the XPS spectra for a $Co_xZn_{1-x}O$ ($x = 0.05$) sample obtained on the as-grown film after removal of 50 Å of surface material by sputtering. Figure 5b shows the binding energy level of Co $2p_{1/2}$ and

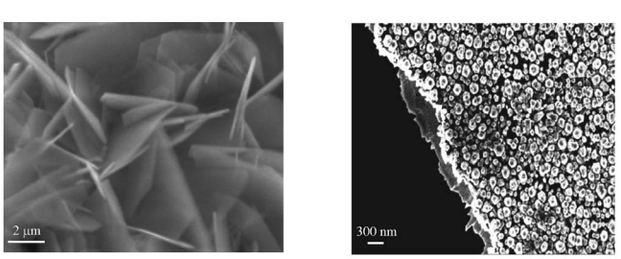

Figure 3. SEMs of $Co_xZn_{1-x}Co$ ($x = 0.05$) electrodeposited on different substrates. (a) Plates with hexagonal shape on polycrystalline gold. (b) Nanopillars with hexagonal shape on Au(111)/Cr/Si(111).

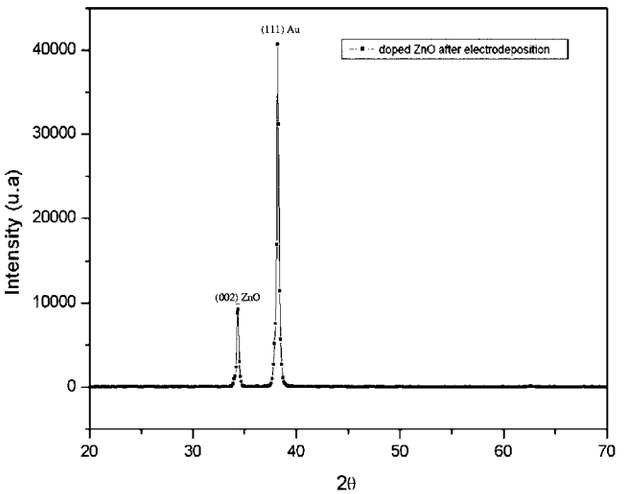

Figure 4. XRD of ZnO thin film deposited on Au(111)/Cr/Si(111).

$2p_{3/2}$ of three samples prepared from three different solution, namely, the first solution contains 3 g/L of $CoSO_4$ with 3 g/L of $NaNO_3$ electrodeposited at −0.8 V, the second solution containing 3 g/L $ZnCl_2$, 3 g/L of $NaNO_3$, 3 g/L of $CoSO_4$ electrodeposited at −0.8 V and finally the same solution as before deposited a −1.0 V. The oxidation state of the Co atoms can be inferred from the shape of the Co 2p lines. The satellite structure on the high binding energy side of the principal $2p_{1/2}$ and $2p_{3/2}$ lines is a typical characteristic of high spin Co^{2+},[17] although the resolution of the XPS measurement is insufficient to resolve multiplet splitting that would delineate the Co spin state. The shake-up peak is a more easily identified characteristic of the chemical state of the Co than either the absolute binding energy or the line separation between Co $2p_{1/2}$ and Co $2p_{3/2}$.[18] Moreover, comparison of the shapes and positions of the primary and shake-up peaks shows that there is a good fit with the film formed by electrodeposition from a solution of $CoSO_4$. By working at higher potential (−1 V), the XP spectra of Co 2p core-line shows that a new peak emerges at 777.8 eV corresponding to Co metallic. To sum up, the characterization shows that the cobalt in the electrodeposited film at −0.8 V is in the +2 oxidation state. It is expected that Co^{+2} would incorporate into the würtzite lattice at Zn^{2+} and Co^{+2}. Thus within the detection limits of the spectrometer, we can rule out metallic Co as the observed source of ferromagnetism. Figure 6 shows typical bright-field TEM images and SAED of the corresponding area from a sample powder of $Zn_{1-x}Co_xO$ (x = 0.06) film electrodeposited at −0.8 V. The bright-field image shows no segregation of $Co(OH)_2$ or Co metallic and reveals the fringes of ZnO{110} with a lattice spacing of about 0.163 nm. The SAED (selected area electron diffraction pattern) inserted in Fig. 6a indicates that the film is a polycrystalline and can be indexed as ZnO hexagonal phase. Figure 6b shows typical bright-field TEM images and SAED of the corresponding area from a sample powder of $Zn_{1-x}Co_xO$ (x = 0.06) film electrodeposited at −1.0 V. The bright-field image shows some large particles of cobalt, they have irregular shapes with concurrent coarsening of the particles in contact with each other. The analyses of the SAED patterns (inset) obtained on the samples shows a predominance of the diffraction rings, which correspond to würtzite ZnO. One more unambiguous diffraction ring has been identified as being metallic Co hexagonal {100}.

Lipinski et al. have already observed electrodeposition of Fe doped with ZnO thin film by working at −0.9 V, the formation of Fe nanoparticles (3–11 nm) embedded in ZnO.[19] By working at higher potential on Co-doped ZnO, we observed the same phenomenon, formation of two phases corresponding of cobalt nanoparticles and hexagonal ZnO. This formation of cobalt aggregates can either be

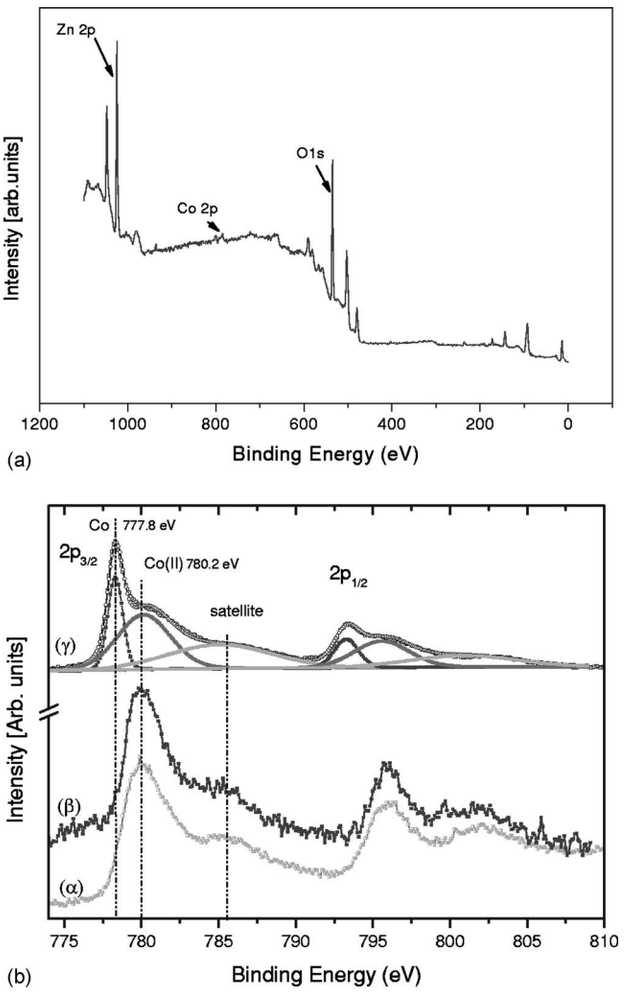

Figure 5. (a) XPS spectra for a $Co_xZn_{1-x}Co$ sample electrodeposited at −0.8 V (after removal 50 Å of surface material by sputtering). (b) (α) XPS spectra of Co2p prepared from a solution of 3 g/L $CoSO_4$ and 2 g/L KNO_3 at 343 K, (β) XPS spectra for an $Co_xZn_{1-x}Co$ (x = 0.05) sample electrodeposited at −0.8 V, γ) XPS spectra for an $Co_xZn_{1-x}Co$ (x = 0.05) sample electrodeposited at −1.0 V.

due to the reduced cobalt ion from the electrolyte and/or by reduction of $Co(OH)_2$ as reported by Foelske et al.[13] Effectively, by forming a superstructure of $Co(OH)_2$ {001} on a single crystal Co{001} single, they observed that a reduction at −1 V will reduce the $Co(OH)_2$ into two-dimensional cobalt metallic structures with the height of one atomic step.

Magnetization study.— Magnetic properties of 6% Co-doped ZnO nanopillar film were measured at temperatures ranging from 5 to 400 K. Figure 7a shows the temperature dependence between the field cooled (FC) and zero field cooled (ZFC) magnetization for the 6% Co-doped ZnO. The ZFC and FC shows the same behavior with the temperature, a ferromagnetism transition up to 350 K. A small decrease in magnetization appears at a temperature higher than 350 K. The same behavior in FC and ZFC can rule out the possibility of cobalt clusters being the origin of the observed ferromagnetic character.[20] At low temperature the magnetization is temperature dependent. This upturn at low temperature shown in Fig. 7a is most likely attributed to the Co moments that remain paramagnetic. The hysteresis loop of the 6% cobalt shows a highly symmetrical aspect with a coercive field of 137 Oe at 3 K. The small 300 K coercivity of only 94 Oe and the resulting small hysteresis

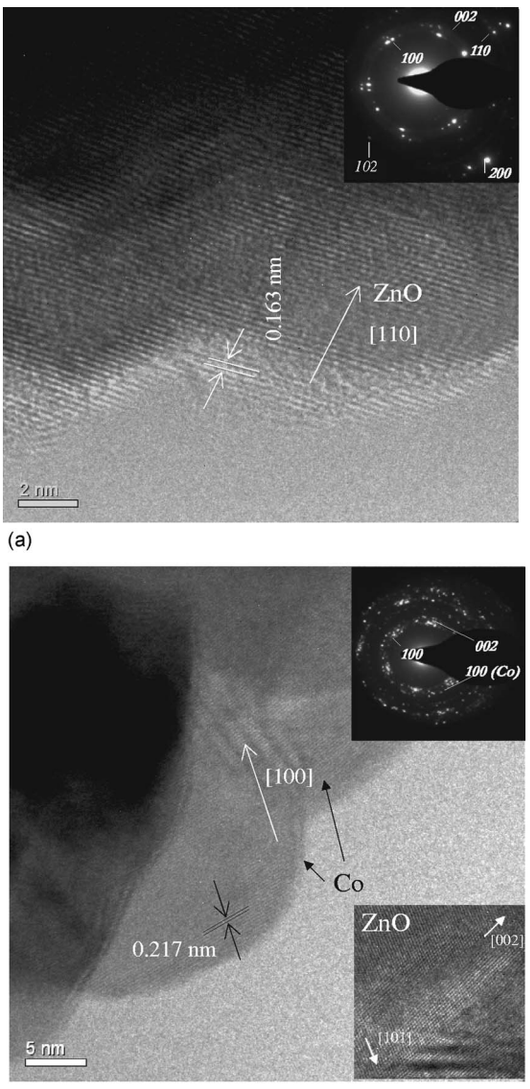

Figure 6. (a) Bright field TEM image showing $Zn_{1-x}Co_xO$ ($x = 0.05$) electrodeposited at −0.8 V. (b) Bright-field TEM image showing $Zn_{1-x}Co_xO$ ($x = 0.05$) electrodeposited at −1 V (the inset corresponding to the SAED pattern and the ZnO bright-field, respectively).

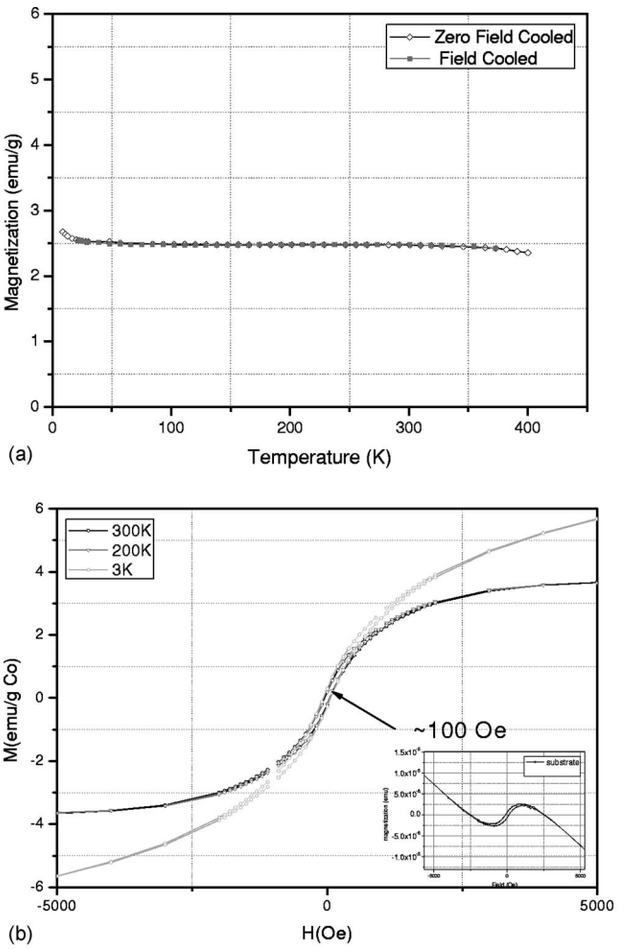

Figure 7. (a) Zero-field-cooling (ZFC) and field-cooling (FC) magnetizations (M) as a function of temperature measured. (b) Hysteresis loops at different temperatures of 3, 200, and 300 K for the $Co_xZn_{1-x}Co$ ($x = 0.05$) electrodeposited hexagonal nanopillar film (inset corresponds to the holder hysteresis and ZnO electrodeposited from a solution of $ZnCl_2$ with $NaNO_3$ at −0.8 V).

area are very similar to those of other ferromagnetic ZnO desorptiom mass spectrometries (DMSs) and nanocrystalline DMS quantum dot aggregates, and characterize these materials as soft ferromagnets. Although the precise origins of the coercivity in these ZnO DMSs remain uncertain, the majority of coercivity likely arises from domain-wall pinning effects. Magnetization was also performed on pure ZnO electrodeposited. This was done to eliminate the possibility that spurious transition metal impurities might be responsible for the magnetic response. The pure ZnO electrodeposited exhibit no hysteresis, showing that the Co doping is responsible for the behavior. The coercive field H_c measured over the same temperature range decreases gradually with the increase of temperature. The gradual decrease in coercivity with increasing temperature is similar to the behavior observed in other ZnO DMSs.[21,22]

Conclusion

In summary, we have presented the preparation, characterization and the magnetic properties of $Co_xZn_{1-x}O$ ($x = 0.05$) nanopillar thin film made by an electrodeposition technique. XPS, HRTEM, ZFC , and FC magnetic susceptibility data are consistent with Co^{2+} ions occupying the cation substitution sites. Ferromagnetism behavior is observed on such electrodeposited materials under aerobic conditions at −0.8 V. XPS shows that under such conditions all the cobalt is in the Co^{2+} oxidation state. This data thus rules out the presence of sufficient cobalt metal to explain the ferromagnetism and instead provide strong experimental support for the existence of intrinsic room-temperature ferromagnetism in Co-doped ZnO. As such, this diluted magnetic semiconductor may indeed be suitable for high-temperature semiconductor spintronics applications.

Ecole Polytechnique Federale de Lausanne assisted in meeting the publication costs of this ariticle.

References

1. S. A. Wolf, *J. Supercond.*, **13**, 195 (2000).
2. G. A. Prinz, *Science*, **282**, 1660 (1998).
3. J. K. Furdyna, *J. Appl. Phys.*, **64**, R24 (1988).
4. T. Dietl, H. Ohno, F. Matsukura, J. Cubert, and D. Ferrand, *Science*, **287**, 1019 (2000).
5. K. Sato and H. Katayama-Yoshida, *Jpn. J. Appl. Phys., Part 2*, **39**, L555 (2000).
6. Y. Matsumoto, M. Murakami, T. Shono, T. Hasegawa, T. Fukumura, M. Kawasaki, P. Ahmet, T. Chikyow, S.-Y. Koshihara, and H. Koinuma, *Science*, **291**, 5505 (2001).
7. P. Sharma, A. Gupta, K. V. Rao, F. J. Owens, R. Sharma, R. Ahuja, J. M. Osorio Guillen, B. Johansson, and G. A. Gehring, *Nat. Mater.*, **2**, 673 (2003).

8. N. S. Norberg, K. R. Kittilstved, J. E. Amonette, R. V. Kukkadapu, D. A. Schwartz, and D. R. Gamelin, *J. Am. Chem. Soc.*, **126**, 9387 (2004).
9. S. Doniach and M. Sunjic, *J. Phys. C*, **3**, 285 (1969).
10. D. A. Shirley, *Phys. Rev. B*, **5**, 4709 (1972).
11. D. Lincot, *Thin Solid Films*, **448**, 40 (2005).
12. J. T. Matsushima, F. Trivinho-Strixino, and E. C. Pereira, *Electrochim. Acta*, **51**, 1960 (2006).
13. A. Foelske, J. Kunze, and H -H. Strehblowa, *Surf. Sci.*, **554**, 10 (2004).
14. T. Pauporte and D. Lincot, *Appl. Phys. Lett.*, **75**, 3817 (1999).
15. R. Liu, A. A. Vertegel, E. W. Bohannan, T. A. Sorensen, and J. A. Switzer, *Chem. Mater.*, **13**, 508 (2001).
16. Z. Jin, *J. Cryst. Growth*, **214/215**, 55 (2000).
17. *Handbook of X-Ray Photoelectron Spectroscopy*, Physical Electronics, Eden Prairie, MN (1995).
18. S. N. Towle, J. R. Bargar, G. E. Brown, Jr., and G. A. Parks, *J. Colloid Interface Sci.*, **187**, 62 (1992).
19. B. B. Lipinski, D. H. Mosca, N. Mattoso, W. H. Schreiner, and A. J. A. De Oliveira, *Electrochem. Solid-State Lett.*, **7**, C115 (2004).
20. Y. Xie and J. Blackman, *J. Phys.: Condens. Matter*, **16**, 4373 (2004).
21. K. Ueda, H. Tabata, and T. Kawai, *Appl. Phys. Lett.*, **79**, 988 (2001).
22. Y. M. Cho, W. K. Choo, H. Kim, D. Kim, and Y. Ihm, *Appl. Phys. Lett.*, **80**, 3358 (2002).